Simulated coordinated impacts of the previous autumn NAO and winter El Niño on the winter aerosol concentrations over eastern China

Juan Feng[1], Jianping Li[2,1], Hong Liao[3], and Jianlei Zhu[4]

1. *College of Global Change and Earth System Science, Beijing Normal University, Beijing, China*
2. *Key Laboratory of Physical Oceanography–Institute for Advanced Ocean Studies, Ocean University of China and Qingdao National Laboratory for Marine Science and Technology, Qingdao 266003, China*
3. *School of Environmental Science and Engineering, Nanjing University of Information Science & Technology, Nanjing, China*
4. *China-ASEAN Environmental Cooperation Center, Beijing, China*

***Corresponding author*:**

Dr. Juan Feng

College of Global Change and Earth System Science (GCESS), Beijing Normal University, Beijing 100875, China

Tel: 86-10-58802762

Email: fengjuan@bnu.edu.cn

Abstract

The high aerosol concentrations (AC) over eastern China have attracted attention from both science and society. Based on the simulations of a chemical transport model using a fixed emissions level, the possible role of the previous autumn North Atlantic Oscillation (NAO) combined with the simultaneous El Niño-South Oscillation (ENSO) on the boreal winter AC over eastern China is investigated. We find that the NAO only manifests its negative impacts on the AC during its negative phase over central China, and a significant positive influence on the distribution of AC is observed over south China only during the warm events of ENSO. The impact of the previous NAO on the AC occurs via an anomalous sea surface temperature tripole pattern by which a teleconnection wave train is induced that results in anomalous convergence over central China. In contrast, the occurrence of ENSO events may induce an anomalous shift in the western Pacific subtropical high and result in anomalous southwesterlies over south China. The anomalous circulations associated with a negative NAO and El Niño are not favorable for the transport of AC and correspond to worsening air conditions over central and south China. The results highlight that the combined effects of tropical and extratropical systems play considerable role in affecting the boreal winter AC over eastern China.

1. Introduction

Atmospheric particles (i.e., aerosols) are the key pollutants that exhibit an important adverse impact on human health, environmental pollution, global climate change, and atmospheric visibility (IPCC, 2013). Aerosol particles may alter the precipitation rates and optical properties of clouds (Hansen et al., 1997), impacting the radiation balance of the entire Earth-atmosphere system via absorbing and scattering solar radiation (Jiang et al., 2017; Yue and Unger, 2017). A better understanding of aerosol variations is therefore important and useful for scientific and social endeavors.

The meteorology parameters, i.e., atmospheric temperature (Aw and Kleeman, 2003; Liao et al., 2015), boundary layer (Kleeman, 2008; Yang et al., 2016), wind (Zhu et al., 2012; Yang et al., 2014, 2017; Feng et al., 2017), and humidity (Ding and Liu, 2014), show a non-negligible impact on the regional aerosol concentrations (AC) via affecting the deposition and transportation processions. Moreover, the intraseasonal and interannual variations in climatic phenomena could affect both the spatial and temporal accumulation and distribution of AC due to the associated variations in the circulation and rainfall anomalies. For example, the monsoon onset could affect the seasonal variations in regional AC (Tan et al., 1998; Chen and Yang, 2008). The interannual variation of AC over East Asia is connected with the interannual variation of East Asian winter monsoon (Jeong and Park, 2016; Lou et al., 2016, 2018; Mao et al., 2017) and summer monsoon (EASM; Zhang et al., 2010; Zhu et al., 2012). The seasonal evolution of the El Niño-South Oscillation (ENSO) impacts the seasonal variations of AC over northern and southern China (Liu et al., 2013; Feng et al., 2016a, 2017). The AC

variation in the US is influenced by the Pacific Decadal Oscillation (Singh and Palazoglu, 2012). These findings suggest that the role of climate systems in impacting the regional air quality cannot be ignored.

The North Atlantic Oscillation (NAO), reflecting large scale fluctuations in pressure between the subpolar low and subtropical high, is one of the most determinant and influential climate variability modes in the extratropical Atlantic Ocean, (e.g., Hurrell, 1995; Gong et al., 2001; Visbeck et al., 2001). A negative (positive) polarity of the NAO is reflected by positive (negative) pressure anomalies over the high latitudes of the North Atlantic and negative (positive) pressure anomalies over the central North Atlantic. Both the positive and negative phases of NAO are accompanied with large scale modulations in the location and intensity of the North Atlantic jet stream and storm track (Gong et al., 2001; Li and Wang, 2003). The surface layer wind would vary associated with changes in the jet stream because of the NAO's quasi-barotropic characteristic, resulting in varied Ekman heat transport and basin-wide variations in the underlying sea surface temperatures (SST; Marshall et al., 2001; Wu et al., 2009; Wu and Wu, 2018).

The NAO massively impacts the temperature and precipitation patterns over the US and central Europe, i.e., a wet and warm winter in Europe, and mild and wet winter conditions would be expected accompanied with a positive NAO phase. Moreover, the NAO exhibits significant cross-seasonal impacts on the downstream regional climate. For example, it is reported that variation in boreal spring NAO influenced the subsequent intensity of the EASM from 1979-2006 (Wu et al., 2009). The linkage

between the EASM and NAO has been further explored but on the interdecadal scale (Wu and Lin, 2012; Wu et al., 2012; Zuo et al., 2013), and it is suggested that the preceding spring NAO dominated the relationship of the NAO-EASM more than the simultaneous summer NAO, similar result is seen in Zheng et al. (2016). Xu et al. (2013) presented that the previous boreal summer NAO significantly influenced the following September rainfall over central China. These studies highlight the important role of the NAO signal on the climate in East Asia, especially the cross-seasonal impacts, which are beneficial for seasonal forecasting.

In addition to the influence of the extratropics, the impact originating from the tropics is another important driver of the climate anomalies in China. As the most dominant interannual variability of the tropical air-sea coupled system, the El Niño-Southern Oscillation (ENSO) exhibits profound influences on the weather and climate around the world (e.g., Ropelewski and Halpert, 1987; Harrison and Larkin, 1998). The occurrence of ENSO phenomenon displays significant effects in impacting the global and regional oceanic and atmospheric anomalous patterns (e.g., Rasmusson and Carpenter, 1982; Trenberth, 1997). The seasonal climate variation in China is closely linked with the evolution of ENSO events. For example, increased rainfall is expected to be found over the Huai-he and Yangtze River valley, whereas less rainfall is seen over northern and southern China during the decaying summer of an El Niño event (Zhang et al., 1996, 1999; Ye and Wu, 2018). During the developing autumn of an El Niño event, enhanced rainfall would be expected over southern China due to the associated anomalous shift in the western Pacific subtropical high (WPSH). However,

without significant influence during the developing summer (Feng et al., 2016b). During the mature winter, both the warm and cold events show significant impacts on the temperature and rainfall anomalies over eastern China (Weng et al., 2009; Wu et al., 2011; Wu and Zhang, 2015; Li et al., 2019; Zhang et al., 2019a, 2019b).

As shown above, both the NAO and ENSO significantly impact the climate over China. China now suffering from relatively high aerosol loading, and this is commonly ascribed to the increased emissions connected with the speedy economic growth. However, as discussed above that the role of meteorological conditions in affecting the AC cannot be ignored. Accordingly, it is of interest to explore the possible impacts of the NAO and ENSO on the distributions of AC over China. The possible impacts of the NAO on the aerosol has been discussed by Moulin et al. (1997) and Jerez et al. (2013); however, they concentrated on its influences on the North Atlantic Ocean and Europe, respectively. Feng et al. (2016a) indicated the potential effects of El Niño on the AC over China, but with a focus on the seasonal evolution. Therefore, does the NAO exhibit significant impacts on the AC, and how the combination of the NAO and ENSO affect the distribution of AC over China, as both of them show important modulation of the climate over China.

The above discussions provide the main motivation of the present work. The conditions in boreal winter are discussed in the present work, as this time is corresponding to the heat supply season and the AC over China peak during this season. The coordinated role of the previous autumn (September to November, SON) NAO and the simultaneous ENSO is compared to that of the NAO alone, and also as well as the

involved physical mechanisms. The rest of this paper is arranged as follows. Model, datasets, and methodology employed are presented in Section 2. The possible impacts of the NAO and ENSO on the AC are explored in Section 3. Section 4 discusses the involved physical mechanism. Section 5 provides the discussion and conclusions.

2. Datasets, simulations, and methodology

2.1 Datasets

The input background meteorological variables of the GEOS-Chem model show high degree of uniformity with the current widely used reanalyses (e.g., Zhu et al., 2012; Yang et al., 2014). Here, the SLP in the National Centers for Environmental Prediction/National Center for Atmospheric Research (NCEP/NCAR) reanalysis (Kalnay et al., 1996) with a 2.5° latitude × 2.5° longitude resolution, and the UK Meteorological Office Hadley Centre's sea ice and SST datasets (HadISST; Rayner et al., 2003) with a 1° latitude × 1° longitude resolution are used to verify the reliability of the Goddard Earth Observing System, Version 4 (GEOS-4).

2.2 GEOS-Chem simulations

The influences of the NAO on the simulated AC over China are examined using a three-dimensional tropospheric chemistry model, i.e., GEOS-Chem (version 8.02.01; Bey et al., 2001). The model is driven by assimilated meteorological fields from the GEOS-4 of the NASA Global Modeling and Assimilation Office, with a 2° latitude × 2.5° longitude resolution, and 30 hybrid vertical levels. This model contains a detailed coupled treatment of tropospheric ozone-NOx-hydrocarbon chemistry, as well as

aerosols and their precursors, containing nitrate, black carbon, sulfate, sea salt, ammonium, mineral dust, dust aerosols, and organic carbon (Bey et al., 2001; Liao et al., 2007). The aerosol dry and wet depositions follow Wesely (1989) and Liu et al. (2001), with details in Wang et al. (1998). According to Liao et al. (2007), the AC were defined as PM2.5 as follows,

$$[PM_{2.5}] = 1.37 \times [SO_4^{2-}] + 1.29 \times [NO_3^-] + [POA] + [BC] + [SOA] \quad (1)$$

SO_4^{2-}, NO_3^-, POA, BC, and SOA are the aerosols particles of sulfate, nitrate, primary organic aerosol, black carbon, and second organic aerosol, respectively. The sea salt aerosols and mineral dust are not considered for that measurements indicate that they are not the major aerosol species in the eastern China during winter (Xuan et al., 2000; Duan et al., 2006).

The anthropogenic emissions in the GEOS-Chem and experiment design are similar to Zhu et al. (2012), in which the biomass burning emissions and anthropogenic emissions are fixed at year 2005 level in the simulation. That is the observed variations in the distributions of AC as seen below was due to the variations in meteorological conditions associated with climate events. Due to the longevity of the GEOS-4 datasets, the period 1986-2006 is focused on. GEOS-Chem is a well-recognized atmospheric chemistry model and is widely utilized due to its capability to well characterize the seasonal, interannual, and decadal variations of pollutant aerosols in the East Asia and beyond (e.g., Zhu et al., 2012; Yang et al., 2014, 2016; Feng et al., 2017). The well performance and wide application of GEOS-Chem provide confidence for employing

the model to investigate the coordinated impacts of NAO and El Niño on the AC over eastern China.

2.3 NAO index and Niño3 index

The NAO index (NAOI) is employed to quantify the variations in the NAO phase (Hurrel et al., 1995; Gong and Wang, 2001). The definition of the NAOI follows Li and Wang (2003) and is calculated as the zonal mean SLP difference between 35°N (i.e., refers to the mid-latitude center) and 65°N (i.e., refers to the high latitude center) from 80°W to 30°E over the North Atlantic by

$$\mathrm{NAOI} = \hat{P}_{35°N} - \hat{P}_{65°N} \tag{2}$$

where P is the monthly mean SLP averaged from 80°W to 30°E, $\hat{P}$ is the normalized value of P, and the subscripts indicate latitudes. For a given month m in year n, the normalization $\hat{P}$ is defined as follows

$$\hat{P}_{n,m} = \frac{P'_{n,m}}{S_P} \tag{3}$$

where $P'_{n,m}$ is the monthly pressure anomaly of $P_{n,m}$, departure from period 1986-2006, and S_P is the total standard deviation of the monthly anomaly $P'_{n,m}$,

$$S_P = \sqrt{\frac{1}{12\times 21}\sum_{i=1986}^{2006}\sum_{j=1}^{12} P'^{2}_{j,i}} \tag{4}$$

The monthly NAOI is calculated based on the monthly mean SLP from both the NCEP/NCAR and GEOS-4 assimilated meteorological dataset for 1986-2006. The boreal autumn NAOI is defined as the average of the monthly NAOI during September, October, and November (Fig. 1). The series of NAOI show strong interannual variations,

194 and the two series based on GEOS-4 and NCEP/NCAR are closely correlated with each
195 other with a significant coefficient of 0.98, implying the GEOS-4 dataset could capture
196 the variation in the NAO.

197 El Niño events were defined as standardized 3-month running mean Niño3 index
198 (areal mean SST averaged over 150°-90°W, 5°N-5°S) above 0.5°C and persisting for at
199 least 6 months. The skin temperature (i.e., SST over ocean and surface air temperature
200 on land) was employed to obtain the Niño3 index for that SST is not available in the
201 GEOS-4 meteorological dataset. The boreal winter Niño3 index is calculated as the
202 average of the monthly Niño3 during December, January, and February, i.e., winter
203 1997 is for the December 1997 and January and February 1998. The boreal winter
204 Niño3 indices based on the GEOS-4 and HadISST are significantly correlated with each
205 other, (Fig. 1), with a coefficient of 0.99. The high correlations among the indices
206 further indicate the reliability of the model data.

207 # 3. Influences of the NAO and El Niño on the AC over China

208 ## 3.1 Climatological Characteristics of the AC

209 The spatial distribution of the standard deviation of boreal winter AC is shown in
210 Fig. 2. Eastern China (105°E eastward, 35°N southward) shows high loading of
211 aerosols in both the column and surface layer concentrations (figure not shown). Further,
212 the variance of winter AC over eastern China is most pronounced compared to other
213 regions during this season (Fig. 2a, b). As an evident monsoonal region, eastern Asia is
214 influenced by winter monsoon, i.e., a strong Aleutian low is seen in the north Pacific,

and the Asian continent is controlled by the Siberian high during boreal winter. The strong pressure gradient between the Siberian high and Aleutian low results in strong northwesterlies prevailing over eastern China (Fig. 2c).

3.2 Relationships between the AC & NAO and El Niño

The spatial distribution between the surface AC and previous autumn NAOI and simultaneous winter Niño3 index are presented in Fig. 3. Positive correlations are seen over south (30°N south) and northwest China in the correlations with the Niño3 index, indicating that a warm ENSO event would associate with high AC over south and northwest China. In contrast, negative correlations over south and central China are observed in the correlations with autumn NAO, implying a positive NAO phase is linked with less AC over these regions, thus favoring better air conditions. The analysis suggests that the ENSO and NAO show opposite effects on AC over south China, i.e., the NAO displays a negative impact and the ENSO displays a positive impact. However, the relationship between the autumn NAOI and winter Niño3 index is insignificant with a correlation of -0.08 during period 1986-2006.

The above relationships are further examined in their positive and negative phases, as strong asymmetry was reported in the climatic impacts of the NAO (Xu et al., 2013; Zhang et al., 2015) and ENSO (Cai and Cowan, 2009; Karior et al., 2013; Feng et al., 2016b). The asymmetric influences of the NAO and ENSO on AC are obvious in the spatial distributions of the linear correlation coefficients (Fig. 4). During the El Niño events, south China is impacted by significant positive correlations, in contrast, a non-

significant correlation is observed over this region during the La Niña events. This point implies the significant relationships between the ENSO and AC over south China are mainly connected with warm events, i.e., El Niño. The negative correlations between the NAO and AC mainly occurred in the negative phase of the NAO, and the significant correlations are mainly located in central China (lie from 28°N to 40°N). Thus, the ENSO affects the distribution of AC in south China, but the impact is manifested during warm events. Similarly, the effect of the NAO on the distribution of AC over central China is only apparent during its negative phase.

The results suggest that if the occurrence of a negative polarity of NAO overlaps with an El Niño event, the combined effects of the two may further worsen the AC over eastern China. In contrast, a solo occurrence of a negative NAO event is associated with above-normal AC over central China. The statistic significant impacts of the negative NAO and El Niño events on the AC could be further established by case study. Two cases, i.e., the co-occurrence of an El Niño event and a negative NAO, and a solo negative NAO event, were chosen to further explore the effect of the NAO and El Niño on the AC over China. From 1986-2006, there are two years (1997 and 2002) with equivalent negative values of autumn NAOI (-1.507 in 1997, and -1.510 in 2002). Winter 1997 corresponds with the strongest El Niño in the past 120 years and winter 2002 corresponds with a neutral ENSO event. Consequently, the anomalous distribution of AC during these two years are discussed in the context of comparing the combined and solo effects of a negative NAO and El Niño in impacting the distribution of AC over eastern China.

3.3 Influences of the NAO & El Niño vs. the NAO on the AC

Figure 5 presents the layer and column AC anomalies simulated for the winters of 1997 and 2002 departure from the climatological mean. Under the combined influence of a negative NAO and El Niño (1997), positive aerosol concentration anomalies are observed over eastern China (Fig. 5a, c). In addition, simulated enhanced AC were observed over central China in winter 2002 under the impacts of a negative NAO (Fig. 5b, d). These characteristics are also apparent in the vertical distribution (Fig. 6), which shows the zonal mean anomalies averaged over eastern China (105°–120°E). For winter 1997, increased AC cover the whole eastern China, with maximum values approximately 30°N, where the effects of the NAO and El Niño overlap (Figs. 4a, d). The combined effects of the anomalies show a consistent distribution in the vertical levels (Fig. 6). In contrast, evident increased AC anomalies are seen in central China, with the maximum at approximately 32°N during winter 2002.

The consistent results between the correlations and anomalies during the two cases highlight the role of the negative NAO and El Niño events in determining the distribution of AC over eastern China. The NAO shows a significant influence on the central China AC that are only apparent during its negative phase, and the ENSO impacts the AC over south China mainly during warm events.

4. Mechanisms of the effects of the NAO and El Niño on the AC

4.1 Role of circulation transport

The corresponding reverse role of the NAO and El Niño in impacting the distribution of AC is mainly derived from their contrasting effects on circulation. Figure 7 shows the SLP and surface wind anomalies during the autumns of 1997 and 2002, presenting an anomalously weak autumn NAO pattern. The negative phase of the NAO displays as an anomalous SLP dipole structure between the middle latitude North Atlantic Ocean and Arctic, i.e., with positive SLP anomalies at the Arctic over the Atlantic sector, and anomalous negative SLP at middle latitude. Although the locations of the anomalous pressure centers in the two negative NAO events show difference, the anomalous SLP amplitude in the two events are similar, i.e., with greater negative SLP anomalies at mid-latitudes, indicating that the pressure gradient of the two NAO negative events is similar. The oscillation in the SLP is connected with anomalies in the surface wind across the North Atlantic, i.e., associated with an anomalous cyclonic centered approximately 45°N and anti-cyclonic circulation anomalies around Iceland. During boreal winter and spring, an anomalous NAO could result in a tripole SST anomalous pattern in the North Atlantic Ocean (Watanabe et al., 1999). A similar SST tripole pattern is observed during boreal autumn, with warm SST anomalies at high and low latitudes, and negative SST anomalies at middle latitudes in the North Atlantic sector (Fig. 8a, c). Note that the negative SST anomalies during 1997 displays an east-west direction but originated from a northwest-southeast direction during 2002 due to the different locations of anomalous SLP (Fig. 7).

The North Atlantic anomalous SST tripole pattern is due to the feedback between wind-SST, i.e., the anomalous anti-cyclonic (cyclonic) circulation weaken (strengthens)

300 the prevailing westerlies, which would result in decreased (increased) loss of heat and
301 warmer (cooler) anomalies in Ekman heat transport (Xie, 2004; Wu et al., 2009), and
302 is connected to warmer (cooler) local SST. Due to the short memory of the atmosphere,
303 the cross-seasonal influences of the NAO on the AC should be preserved in the
304 boundary layer forcing such as SST (Charney and Shukla, 1981). This anomalous
305 tripole SST pattern could persist to the following winter (Fig. 8b, d), as the anomalous
306 tripole SST pattern during winter and autumn show high consistencies in both 1997 and
307 2002, with significant spatial correlation coefficients of 0.32 and 0.51 between the
308 autumn and winter tripole SST patterns for 1997 and 2002, respectively.

309 Figure 9 shows the anomalous divergence at the upper troposphere. The
310 occurrence of a negative NAO phase is accompanied by an anomalous teleconnection
311 wave train over northern Eurasia (AEA) in the upper troposphere during boreal summer
312 (Li and Ruan, 2018). This anomalous teleconnection pattern is also observed during
313 boreal winter, with a shift in the precise locations. Under the influence of the anomalous
314 downstream teleconnection, north China is influenced by convergence anomalies, with
315 the center positioned over central China (Fig. 9). The anomalous convergence is clearly
316 seen in both the upper and lower troposphere, accompanied by anomalous easterlies or
317 southeasterlies over central China (Fig. 10). The direction of the anomalous wind is
318 opposite to the climatological winds, which would weaken the climatological wind and
319 is unfavorable for the transport of aerosol concentration, leading to increased AC over
320 central China, as displayed in Fig. 5.

For the winter 1997, corresponding to the El Niño's mature phase, south China was influenced by an evident anomalous divergence at the lower troposphere, indicating anomalous anticyclonic circulation over the coastal regions (Fig. 10a). Anomalous southwesterlies prevailed in south China, implying weakened northerlies. That is the anomalous meteorological conditions are unfavorable for aerosols transport in the region and would result in a worsen air quality. In contrast, for the winter 2002, south China was controlled by an anomalous divergence for that the main body of the WPSH shifts to the south of south China (Fig. 10b). The anomalous circulation was favorable for the emission of pollutant. Moreover, an evident anomalous divergence was observed in south China in the winters of 1997 and 2002 at the upper troposphere; however, the corresponding distribution of AC over this region is different. This highlights the role of El Niño in impacting the circulation anomalies over south China, as mentioned above. The occurrence of El Niño events would be accompanied by a northwest shift of the WPSH during boreal winter and enhanced southwesterlies over south China (Weng et al., 2009). Besides, column AC are mainly contributed by concentrations at lower troposphere, suggesting that the lower troposphere circulation may play a vital role in impacting the AC over south China.

4.2 Role of wet deposit

In addition to the contribution of the circulation anomalies to the distribution of AC, changes in wet deposit also could affect distribution of AC. Figure 11 presents the simulated wet deposit anomalies during the winters of 1997 and 2002. Negative anomalies occurred over eastern China during the winter of 1997, favorable for

343 increased AC. This suggests the wet deposit plays a positive role in the enhanced AC
344 during winter 1997. Positive anomalies were observed over central China in the 2002
345 winter, inconsistent with the AC anomalies. The anomalous wet deposit during winter
346 of 1997 is paralleling to the AC anomalies over eastern China; however, not consistent
347 with that for the winter of 2002. This suggests that role of wet deposit in impacting the
348 AC over eastern China exists uncertainties, showing strong regional dependence. The
349 impact of wet deposit on the AC was examined by a sensitive experiment by turning
350 off the wet deposition (Fig. 11c-d). A similar anomalous AC distribution was observed
351 as those shown in Fig. 5, confirming that the role of wet deposit in impacting the
352 distribution of AC is not as important as the circulation.

353 ## 5. Summary and Discussion

354 Using the simulations of GEOS-Chem model with fixed emissions, the
355 coordinated impacts of the previous autumn NAO and simultaneous ENSO on the
356 boreal winter AC over eastern China are investigated. The results present that both the
357 NAO and ENSO show asymmetry impacts on the boreal winter AC over eastern China,
358 i.e., the NAO manifests negative impacts over central China during its negative phase
359 and the ENSO positively impacts the AC over south China significantly during its warm
360 events. Consequently, the possible impacts of two cases were investigated to ascertain
361 the role of the NAO and ENSO on the distribution of AC over China. The winter 1997
362 had a co-occurrence of a negative NAO and an El Niño events, and winter 2002
363 corresponds to a negative NAO phase and neutral ENSO. For the winter 1997, obvious
364 enhanced AC were observed over eastern China, with a maximum approximately 30°N,

where the impacts of the NAO and El Niño overlap. For the winter 2002, there were generally increased AC over central China. These results suggest that the co-occurrence of a negative NAO and El Niño would worsen the air conditions over eastern China, and a solo negative NAO is associated with increased AC over central China.

The cross-seasonal impacts of the preceding autumn NAO on the following winter AC over China can be explained by the coupled air-sea bridge theory (Li and Ruan, 2018). The preceding negative NAO exhibits significant influences on the winds due to the adjustment of the wind to the anomalous SLP. The associated anomalous wind could affect the underlying regional SST, resulting in an anomalous SST tripole pattern over the North Atlantic. Since the North Atlantic SST exhibit strong persistence, this anomalous SST pattern could persist to the subsequent winter and inducing an anomalous AEA teleconnection wave train in the upper troposphere, with anomalous convergence over central China. Thus, central China is controlled by anomalous southeasterlies or easterlies, which weaken the climatological northwesterlies and induce increased AC over central China. In contrast, the occurrence of El Niño is linked to warm SST anomalies over tropical eastern Pacific, by which the Rossby wave activity would be altered (Wang et al., 2001; Feng and Li, 2011). A northwest shift of the WPSH is seen during the winter of an El Niño event, associated with southwesterlies anomalies over south China during the winter of 1997, indicating a weakening in the climatological wind and leading to enhanced AC over south China. Therefore, the high level of AC over eastern China during the winter 1997 results from the combined role

386 of the NAO and El Niño, and the high concentrations over central China in the winter
387 of 2002 are attributed to the NAO.

388 The possible reason for the asymmetric influence of the NAO on the AC was
389 further explored. When the autumn NAO is in the positive polarity, for example, two
390 positive cases of 1986 and 1992, the associated underlying SST anomalies (figure not
391 shown), particularly the tripole SST pattern, are not as evident as those shown in the
392 negative NAO. This result may provide a possible explanation for the asymmetric
393 relationship existed in the different phases of the NAO and AC, and implies the
394 complexity of the atmosphere-ocean feedback in the North Atlantic. This merits further
395 exploration related to why the linkage between the NAO and underlying SST is
396 nonlinear, and what process is responsible for their nonlinear relationship.

397 As noted above, the influence of the NAO on the AC only manifests during its
398 negative phase, and the impact of the ENSO is only significant during its warm events.
399 However, the relationship between the previous autumn and following winter ENSO is
400 insignificant, thus it is of interest to establish the nonlinear relationship among them
401 and investigate why there is strong asymmetry in the relationships. Zhang et al. (2015,
402 2019) explored the complex linkage between the boreal winter NAO and ENSO with
403 the former lagged for one month, indicating that the nonlinear relationship of the NAO
404 and ENSO is modulated by the interdecadal variation in the Atlantic Multi-Decadal
405 Oscillation. In addition, Wu et al. (2009) have illustrated the coordinated impacts of the
406 NAO and ENSO in modulating the interannual variation of the EASM; however, it has
407 not been shown to determine the AC yet. Therefore, it is of interest to further explore

whether the NAO and ENSO affect the AC over China in other seasons, as well as the process involved. Furthermore, the present work is based on model simulations and due to the limitations of the model simulations, only the interannual variations are considered. As both NAO and ENSO show strong interdecadal variations, for a longer period, i.e., 1850-2017 (figure not shown), the NAO during period 1986-2006 is generally located in the positive phase, whereas in the negative phase during period 1955-1970, therefore, it is important to determine the interdecadal modulation of the NAO on the distribution of AC.

Moreover, the role of rainfall in influencing the AC shows uncertainties, i.e., a positive effect over south China but not for central China. This result is similar with that of Wu (2014), showing the impact of wet deposit on the AC shows regional and seasonal dependence. This is may due to the fact that the climatological winter rainfall over central China is much less than that over south China (figure not shown). In addition, the meteorological backgrounds of south China and central China are different, baroclinic over central China and barotropic over south China (Fig. 9 vs. 10), indicating the importance of climatology background in impacting the spatial distribution of AC. In addition, both the NAO and ENSO show significant correlations with AC over northwest China (Fig. 4); however, the interannual variation (Fig. 2) and anomalies (Fig. 5) in AC over those regions are relatively small. Therefore, the AC variation over those regions are not discussed.

Finally, the role of NAO and El Niño on the AC during boreal winter was investigated based on GEOS-Chem simulations. The coordinated role of the NAO and

El Niño in affecting the distribution of AC over eastern China is highlighted by comparing this effect with the solo role of the NAO. The result indicates that the influence of meteorological factors impacting AC is complicated. Future work will investigate the combined role of tropical and extratropical signals on seasonal AC to better understand the variation across seasons and to determine the possible contribution of natural variability to the current aerosol loading over China.

Author contribution

J. F., J. L., and H. L. designed the research. J. F. and J. Z. performed the data analysis and simulations. J. F. led the writing and prepared all figures. All the authors discussed the results and commented on the manuscript.

Data availability

The HadISST dataset is available online at http://www.metoffice.gov.uk/hadobs/hadisst/data/download.html. The NCEP/NCAR reanalyses is available at http://www.esrl.noaa.gov/psd/data/gridded/. The model output used in the figures of this study is available at Zenodo (https://doi.org/10.5281/zenodo.3247326).

Acknowledgement

This work was jointly supported by the National Natural Science Foundation of China (41790474, 41705131, and 41530424).

References

Aw, J., and Kleeman, M. J.: Evaluating the first-order effect of intra-annual temperature variability on urban air pollution, J. Geophys. Res. Atmos., 108, D12, 4365, https://doi.org/10.1029/2002JD002688, 2003.

Bey, I., Jacob, D. J., Yantosca, R. M., Logan, J. A., Field, B. D., Fiore, A. M., Li, Q. B., Liu, H. Y., Mickley, L. J., and Schultz, M. G.: Global modeling of tropospheric chemistry with assimilated meteorology: Model description and evaluation, J. Geophys. Res., 106, 23073-23095, https://doi.org/10.1029/2001JD000807, 2001.

Cai, W. J., and Cowan, T.: La Niña Modoki impacts Australia autumn rainfall variability, Geophys. Res. Lett., 36, L12805, https://doi.org/10.1029/2009GL037885, 2009.

Chen, B. Q., and Yang Y. M.: Remote sensing of the spatio-temporal pattern of aerosol over Taiwan Strait and its adjacent sea areas, Acta Scientiae Circumstantiae, 28, 12, 2597-2604, 2008.

Duan, F. K., He, K. B., Ma, Y. L., Yang, F. M., Yu, X. C., Cadle, S. H., Chan, T., and Mulawa, P. A.: Concentration and chemical characteristics of PM2.5 in Beijing, China: 2001-2002, Sci. Total Environ., 355, 264–275, https://doi.org/10.1016/j.scitotenv.2005.03.001, 2006.

Feng, J., and Li, J. P.: Influence of El Niño Modoki on spring rainfall over south China, J. Geophys. Res. Atmos., 116, D13102, https://doi.org/10.1029/2010JD015160, 2011.

Feng, J., Zhu, J. L., and Li, Y.: Influences of El Niño on aerosol concentrations over eastern China, Atmos. Sci. Lett., 17, 422-430, https://doi.org/10.1002/asl.674,

2016a.

Feng, J., Li, J. P., Zheng, F., Xie, F., and Sun, C.: Contrasting impacts of developing phases of two types of El Niño on southern China rainfall, J. Meteorol. Soc. Jap., 94, 359-370, https://doi.org/10.2151/jmsj.2016-019, 2016b.

Feng, J., Li, J. P., J. Zhu, J. L., Liao, H., and Yang, Y.: Simulated contrasting influences of two La Niña Modoki events on aerosol concentrations over eastern China, J. Geophys. Res. Atmos., 122, https://doi.org/10.1002/2016JD026175, 2017.

Gong, D. Y., Wang, S. W., and Zhu, J. H.: East Asian winter monsoon and Arctic Oscillation, Geophys. Res. Lett., 28, 2073-2076, https://doi.org/10.1029/2000GL012311, 2001.

Hansen, J., Sato, M., and Ruedy, R.: Radiative forcing and climate response, J. Geophys. Res., 102, D6, 6831-6864, https://doi.org/10.1029/96JD03436, 1997.

Harrison, D. E., and Larkin, N. K.: Seasonal U.S. temperature and precipitation anomalies associated with El Niño: Historical results and comparison with 1997-98, Geophys. Res. Lett., 25, 3959–3962, https://doi.org/10.1029/1998GL900061, 1998.

Hurrell, J. W.: Decadal trends in the North Atlantic Oscillation: Regional temperature and precipitation, Science, 269, 676-679, doi:10.1126/science.269.5224.676, 1995.

IPCC, Climate change.: The physical science basis. Cambridge University Press. Cambridge, UK, 2013.

Jeong, J. I., and Park, R. J.: Winter monsoon variability and its impacts on aerosol concentrations in East Asia, Environ. Poll., 221, 285-292,

https://doi.org/10.1016/j.envpol.2016.11.075, 2017.

Jerez, S., Jimenez-Guerrero, P., Montavez, J. P., and Trigo, R. M.: Impact of the North Atlantic Oscillation on European aerosol ground levels through local processes: a seasonal model-based assessment using fixed anthropogenic emissions, Atmos. Chem. Phys., 13, 11195-11207, https://doi.org/10.5194/acp-13-11195-2013, 2013.

Jiang, Y. Q., Yang, X. Q., Liu, X. H., Yang, D. J., Sun, X. G., Wang, M. H., Ding, A. J., Wang, T. J., and Fu, C. B.: Anthropogenic aerosol effects on East Asian winter monsoon: The role of black carbon-induced Tibetan Plateau warming, J. Geophys. Res. Atmos., 122, 5883-5902, https://doi.org/10.1002/2016JD026237, 2017.

Kalnay, E., Kanamitsu, M., Kistler, R., Colliins, W., Deaven, D., Gandin, L., Iredell, M., Saha, S., White, G., Woollen, J., Zhu, Y., Chelliah, M., Ebisuzaki, W., Higgins, W., Janowiak, J., Mo, K. C., Ropelewski, C., Wang, J., Leetmaa, A., Reynolds, R., Jenne, R., and Joseph, D.: The NCEP/NCAR 40-Year Reanalysis Project, Bull. Amer. Meteor. Soc., 77, 437-472, https://doi.org/10.1175/1520-0477(1996)077<0437:TNYRP>2.0.CO;2, 1996.

Karori, M. A., Li, J. P., and Jin, F. F.: The asymmetric influence of the two types of El Niño and La Niña on summer rainfall over southeast China, J. Climate, 26, 4567-4582, https://doi.org/10.1175/JCLI-D-12-00324.1, 2013.

Kleeman, M.: A preliminary assessment of the sensitivity of air quality in California to global change. Climate Change, 87, 273-292, https://doi.org/10.1007/s10584-007-9351-3, 2008.

Li, J. P., and Ruan, C. Q.: The North Atlantic–Eurasian teleconnection in summer and

its effects on Eurasian climates. Environ. Res. Lett., 13, https://doi.org/10.1088/1748-9326/aa9d33, 2018.

Li, J. P., and Wang, J. X. L.: A new North Atlantic Oscillation index and its variability, Adv. Atmos. Sci., 20, 661-676, https://doi.org/10.1007/BF02915394, 2003.

Li, K., Liao, H., Cai, W. J., and Yang, Y.: Attribution of anthropogenic influence on atmospheric patterns conducive to recent most severe haze over eastern China, Geophys. Res. Lett., 45, 2072-2081, https://doi.org/10.1002/2017GL076570, 2018.

Li, Y., Ma, B. S., Feng, J., and Lu, Y.: Influence of the strongest central Pacific ENSO events on the precipitation in eastern China, Int. J. Climatol., https://doi.org/10.1002/joc.6004, 2019.

Liao, H., Henze, D. K., Seinfeld, J. H., Wu, S. L., and Mickley, L. J.: Biogenic secondary organic aerosol over the United States: Comparison of climatological simulations with observations, J. Geophys. Res., 112, https://doi.org/10.1029/2006JD007813, 2007.

Liao, H., Chang, W., and Yang, Y.: Climatic effects of air pollutants over China: A review, Adv. Atmos. Sci., 32, 115-139, doi:10.1007/s00376-014-0013-x, 2015.

Liu, H., Jacob, D. J., Bey, I., and Yantosca, R. M.: Constraints from 210Pb and 7Be on wet deposition and transport in a global three-dimensional chemical tracer model driven by assimilated meteorological fields, J. Geophys. Res., 106, 12109-12128, https://doi.org/10.1029/2000JD900839, 2001.

Lou, S. J., Russell, L. M., Yang, Y., Xu, L., Lamjiri, M. A., DeFlorio, M. J., Miller, A.

539 J., Ghan, S. J., Liu, Y., and Singh, B.: Impacts of the East Asian monsoon on
540 springtime dust concentrations over China, J. Geophys. Res. Atmos., 121, 8137-
541 8152, https://doi.org/10.1002/2016JD024758, 2016.
542 Lou, S. J., Yang, Y., Wang, H. L., Smith, S. J., Qian, Y., Rasch, P. J.: Black carbon amplifies
543 haze over the North China Plain by weakening the East Asian winter monsoon, Geophys.
544 Res. Lett., 45, https://doi.org/10.1029/2018GL080941, 2018.
545 Mao, Y. H., Liao, H., and Chen H. S.: Impacts of East Asian summer and winter
546 monsoons on interannual variations of mass concentrations and direct radiative
547 forcing of black carbon over eastern China, Atmos. Chem. Phys., 17, 4799-4816,
548 https://doi.org/10.5194/acp-17-4799-2017, 2017.
549 Marshall, J., Johnson, H., and Goodman, J.: A study of the interaction of the North
550 Atlantic Oscillation with ocean circulation, J. Climate, 14, 1399–1421,
551 https://doi.org/10.1175/1520-0442(2001)014<1399:ASOTIO>2.0.CO;2, 2001.
552 Moulin, C., Lambert, C. E., Dulac, F., and Dayan, U.: Control of atmospheric export of
553 dust from North Atlantic by the North Atlantic Oscillation, Nature, 3877, 691-694,
554 https://doi.org/10.1038/42679, 1997.
555 Park, R. J., Jacob, D. J., Chin, M., and Martin, R. V.: Sources of carbonaceous aerosols
556 over the United States and implications for natural visibility, J. Geophys. Res., 108,
557 4355, https://doi.org/10.1029/2002JD003190, 2003.
558 Park, R. J., Jacob, D. J., Field, B. D., Yantosca, R. M., and Chin, M.: Natural and
559 transboundary pollution influences on sulfate-nitrate-ammonium aerosols in the
560 United States: implications for policy, J. Geophys. Res., 109, D15204,

https://doi.org/10.1029/2003JD004473, 2004.

Park, R. J., Jacob, D. J., Kumar, N., and Yantosca, R. M.: Regional visibility statistics in the United States: natural and transboundary pollution influences, and implications for the regional haze rule, Atmos. Environ., 40, 5405-5423, https://doi.org/10.1016/j.atmosenv.2006.04.059, 2006.

Qin, Y., Chan, C. K., and Chan, L. Y.: Characteristics of chemical compositions of atmospheric aerosols in Hongkong: spatial and seasonal distributions, Science of the total Environment, 206, 25-37, https://doi.org/10.1016/S0048-9697(97)00214-3, 1997.

Qiu, Y. L., Liao, H., Zhang, R. J., and Hu, J. L.: Simulated impacts of direct radiative effects of scattering and absorbing aerosols on surface-layer aerosol concentrations in China during a heavily polluted event in February 2014, J. Geophys. Res., 122, 5955-5975, https://doi.org/10.1002/2016JD026309, 2017.

Rasmusson, E. M., and Carpenter, T. H.: Variations in tropical sea surface temperature and surface wind fields associated with the Southern Oscillation/El Niño, Mon. Wea. Rev., 110, 354-384, https://doi.org/10.1175/1520-0493(1982)110<0354:VITSST>2.0.CO;2, 1982.

Rayner, N. A., Parker, D. E., Horton, E. B., Folland, C. K., Alexander, L. V., and Rowell, D. P.: Global analyses of sea surface temperature, sea ice, and night marine air temperature since the late nineteenth century, J. Geophys. Res., 108, D14, 4407, https://doi.org/10.1029/2002JD002670, 2003.

Ropelewski, C. F., and Halpert, M. S.: Global and regional scale precipitation patterns

583 associated with the El Niño/Southern Oscillation, Mon. Wea. Rev., 115, 1606-
584 1626, http://dx.doi.org/10.1175/1520-0493(1987)115<1606:GARSPP>2.0.CO;2,
585 1987.
586 Singh, A., and Palazoglu, A.: Climatic variability and its influence on ozone and PM
587 pollution in 6 non-attainment regions in the United States, Atmos. Environ., 51,
588 212–224, doi:10.1016/j.atmosenv.2012.01.020, 2012.
589 Trenberth, K. E.: The definition of El Niño, Bull. Amer. Meteor. Soc., 78, 2771-2777,
590 https://doi.org/10.1175/1520-0477(1997)078<2771:TDOENO>2.0.CO;2, 1997.
591 Visbeck, M. H., Hurrell, J. W., Polvani, L., and Cullen, H. M.: The North Atlantic
592 Oscillation: past, present, and future, PNAS, 98, 12876-12877,
593 https://doi.org/10.1073/pnas.231391598, 2001.
594 Wang, B., Wu, R. G., and Fu, X. H.: Pacific–East Asian teleconnection: how does
595 ENSO affect East Asian Climate? J. Climate, 13, 1517-1536,
596 https://doi.org/10.1175/1520-0442(2000)013<1517:PEATHD>2.0.CO;2, 2000.
597 Wang, Y. H., Jacob, D. J., and Logan, J. A.: Global simulation of tropospheric O3-NO
598 x-hydrocarbon chemistry 1. model formulation, J. Geophys. Res., 103, 10713,
599 https://doi.org/10.1029/98JD00158, 1998.
600 Watanabe, M., and Nitta, T.: Decadal changes in the atmospheric circulation and
601 associated surface climate variations in the Northern Hemisphere winter, J. Climate,
602 12, 494-509, https://doi.org/10.1175/1520-
603 0442(1999)012<0494:DCITAC>2.0.CO;2, 1999.
604 Weng, H. Y., Behera, S. K., and Yamagata, T.: Anomalous winter climate conditions in

the Pacific rim during recent El Niño Modoki and El Niño events, Clim. Dyn., 32, 663-674, https://doi.org/10.1007/s00382-008-0394-6, 2009.

Wesely, M. L.: Parameterization of surface resistances to gaseous dry deposition in regional-scale numerical models, Atmos. Environ., 23, 1293-1304, https://doi.org/10.1016/0004-6981(89)90153-4, 1989.

Wu, J., and Wu, Z. W.: Interdecadal change of the spring NAO impact on the summer Pamir-Tienshan snow cover, Int. J. Climatol., 39, 629-642, https://doi.org/10.1002/joc.5831, 2018.

Wu, R. G.: Seasonal dependence of factors for year-to-year variations of South China aerosol optical depth and Hong Kong air quality, Int. J. Climatol., 34, 3204-3220, doi:10.1002/joc.3905, 2014.

Wu, Z. W., Wang, B., Li, J. P., and Jin, F.-F.: An empirical seasonal prediction model of the east Asian summer monsoon using ENSO and NAO, J. Geophys. Res., 114, D18120, https://doi.org/10.1029/2009JD011733, 2009.

Wu, Z. W., Li, J. P., Jiang, Z. H., He, J. H., and Zhu, X. Y.: Possible effects of the North Atlantic Oscillation on the strengthening relationship between the East Asian summer monsoon and ENSO, Int. J. Climatol., 32, 794-800, https://doi.org/10.1002/joc.2309, 2012.

Wu, Z. W., and Lin, H.: Interdecadal variability of the ENSO-North Atlantic Oscillation connection in boreal summer, Q. J. Roy. Meteor. Soc., 138, 1668-1675, https://doi.org/10.1007/s00382-014-2361-8, 2012.

Wu, Z. W., Li, J. P., Jiang, Z. H., and He, J. H.: Predictable climate dynamics of

627 abnormal East Asian winter monsoon: once-in-a-century snowstorms in
628 2007/2008 winter, Clim. Dyn., 37, 1661-1669, https://doi.org/10.1007/s00382-
629 010-0938-4, 2011.
630 Wu, Z. W., and Zhang, P.: Interdecadal variability of the mega-ENSO-NAO
631 synchronization in winter, Clim. Dyn., 45, 1117-1128,
632 https://doi.org/10.1007/s00382-014-2361-8, 2015.
633 Xie, S. P.: Satellite observations of cool ocean–atmosphere interaction, Bull. Amer.
634 Meteor. Soc., 85, 195-208, https://doi.org/10.1175/BAMS-85-2-195, 2004.
635 Xu, H. L., Feng, J., and Sun, C.: Impact of preceding summer North Altantic Oscillation
636 on early autumn precipitation over central China, Atmos. Oceanic Sci. Lett., 6, 417-
637 422, https://doi.org/10.3878/j.issn.1674-2834.13.0027, 2013.
638 Xuan, J., Liu, G. L., and Du, K.: Dust emission inventory in northern China, Atmos.
639 Environ., 34, 4565–4570, https://doi.org/10.1016/S1352-2310(00)00203-X, 2000.
640 Yang, Y., Liao, H., Li, J.: Impacts of the East Asian summer monsoon on interannual
641 variations of summertime surface-layer ozone concentrations over China, Atmos.
642 Chem. Phys., 14, 6867-6879, https://doi.org/10.5194/acp-14-6867-2014, 2014.
643 Yang, Y., Liao, H., and Lou, S. J.: Increase in winter haze over eastern China in the past
644 decades: Roles of variations in meteorological parameters and anthropogenic
645 emissions, J. Geophys. Res. Atmos., 121, 13050-13065,
646 https://doi.org/10.1002/2016JD025136, 2016.
647 Yang, Y., Russell, L. R., Lou, S. J., Liao, H., Guo, J. P., Liu, Y., Singh, B., and Ghan, S.
648 J.: Dust-wind interactions can intensify aerosol pollution over eastern China,

649 Nature Comm., 8, 15333, https://doi.org/10.1038/ncomms15333, 2017.
650 Ye, X., and Wu, Z. W.: Contrasting impacts of ENSO on the interannual variations of
651 summer runoff between the upper and mid-lower reaches of the Yangtze river,
652 Atmosphere, 9, 478, https://doi.org/10.3390/atmos9120478, 2018.
653 Yue, X., and Unger, N.: Aerosol optical depth thresholds as a tool to assess diffuse
654 radiation fertilization of the land carbon uptake in China, Atmos. Chem. Phys., 17,
655 1329-1342, https://doi.org/10.5194/acp-17-1329-2017, 2017.
656 Zhang, L., Liao, H., and Li, J. P.: Impacts of Asian summer monsoon on seasonal and
657 interannual variations of aerosols over eastern China, J. Geophys. Res., 115,
658 D00K05, https://doi.org/10.1029/2009JD012299, 2010.
659 Zhang, P., Wang, B., and Wu, Z. W.: Weak El Niño and winter climate in the mid-high
660 latitude Eurasia, J. Climate, 32, 402-421, https://doi.org/10.1175/JCLI-D-17-
661 0583.1, 2019a.
662 Zhang, P., Wu, Z. W., and Li, J. P.: Reexamining the relationship of La Niña and the
663 East Asian winter monsoon, Clim. Dyn., https://doi.org/10.1007/s00382-019-
664 04613-7, 2019b.
665 Zhang, P., Wu, Z. W., and Chen H.: Interdecadal modulation of mega-ENSO on the
666 north Pacific atmospheric circulation in winter, Atmos. Ocean, 55, 110-120,
667 https://doi.org/10.1080/07055900.2017.1291411, 2017.
668 Zhang, R., Sumi, A., and Kimoto, M.: Impact of El Niño on the East Asian monsoon:
669 A Diagnostic Study of the '86/87' and '91/92' events, J. Meteorol. Soc. Jpn., 74,
670 49–62, https://doi.org/10.2151/jmsj1965.74.1_49, 1996.Zhang, R. H., Sumi, A.,

671 and Kimoto, M.: A diagnostic study of the impact of El Niño on the precipitation
672 in China, Adv. Atmos. Sci., 16, 229-241, https://doi.org/10.1007/BF02973084,
673 1999.
674 Zhang, W. J., Wang, L., Xiang, B. Q., He, J. H.: Impacts of two types of La Niña on the
675 NAO during boreal winter, Clim. Dyn., 44, 1351-1366,
676 https://doi.org/10.1007/s00382-014-2155-z, 2015.
677 Zhang, W. J., Mei, X. B., Geng, X., Turner, A. G., and Jin, F.-F.: A nonstationary ENSO-
678 NAO relationship due to AMO modulation, J. Climate, 32, 33-43,
679 https://doi.org/10.1175/JCLI-D-18-0365.1, 2019.
680 Zheng, F., Li, J. P., Li, Y. J., Zhao, S., and Deng, D. F.: Influence of the Summer NAO
681 on the Spring-NAO-Based Predictability of the East Asian Summer Monsoon, J.
682 App. Meteorol. Climatol., 55, https://doi.org/10.1175/JAMC-D-15-0199.1, 2016.
683 Zhu, J. L., Liao, H., and Li, J. P.: Increases in aerosol concentrations over eastern China
684 due to the decadal-scale weakening of the East Asian summer monsoon, Geophys.
685 Res. Lett., 39(9), L09809, https://doi.org/10.1029/2012GL051428, 2012.
686 Zuo, J. Q., Li, W. J., Sun, C. H., Xu, L., and Ren, H. L.: Impact of the North Atlantic
687 sea surface temperature tripole on the East Asian summer monsoon, Adv. Atmos.
688 Sci., 30, 1173-1186, https://doi.org/10.1007/s00376-012-2125-5, 2013.
689

690 # Figure Captions:

691 **Figure 1**. (a) The time series of the Niño3 index based on the GEOS-4 input skin
692 temperature data for 1986-2006 (°C). (b) is similar to (a) but is based on the
693 HadISST. (c) The time series of the NAO index based on the GEOS-4 input sea
694 level pressure. (d) is similar to (c) but is based on the NCEP/NCAR reanalysis.

695 **Figure 2**. The standard deviation of the simulated (a) surface layer $PM_{2.5}$ concentrations
696 ($\mu g \cdot m^{-3}$) and (b) column burdens of $PM_{2.5}$ ($mg \cdot m^{-2}$) during boreal winter averaged
697 from 1986 to 2006. (c) The horizontal distribution of boreal winter climatological
698 mean wind at 850 hPa ($m \cdot s^{-1}$), shaded indicates the Tibetan Plateau.

699 **Figure 3**. (a) The spatial distribution of the correlation coefficients between surface
700 layer $PM_{2.5}$ concentrations and the Niño3 index. (b) As in (a), but for the
701 correlations with the NAOI. Color shading indicates a significant correlation at the
702 0.1 level (0.37 is the critical value for significance at the 0.1 level).

703 **Figure 4**. Spatial distribution of the correlation coefficients between (a) positive and (b)
704 negative Niño3 index values and surface-layer $PM_{2.5}$ concentrations. (c)-(d) as in
705 (a)-(b), but for the NAOI. Color shading indicates a significant correlation, (0.35
706 and 0.45 are the critical value for significance at the 0.2 and 0.1 level, respectively).

707 **Figure 5**. The spatial distribution of the simulated anomalous (left panel) surface layer
708 $PM_{2.5}$ concentrations ($\mu g \cdot m^{-3}$) and (right panel) column burdens of $PM_{2.5}$ ($mg \cdot m^{-2}$)
709 during the boreal winters of 1997 (upper) and 2002 (below).

710 **Figure 6**. The pressure–latitude distribution of zonally averaged $PM_{2.5}$ anomalies over
711 105°–120°E during the winters of (a)1997 and 2002 ($\mu g \cdot m^{-3}$).

712 **Figure 7**. The horizontal distribution of surface wind ($m \cdot s^{-1}$) and surface level pressure
713 (hPa) based on the assimilated meteorological data during the autumns of (a) 1997
714 and (b) 2002.
715 **Figure 8**. The horizontal distribution of skin temperature anomalies (°C) based on the
716 assimilated meteorological data during the (a) autumn and (b) winter of 1997. (c)-
717 (d) As in (a)-(b), but during 2002.
718 **Figure 9**. Horizontal distribution of the divergence ($10^{-5}s^{-1}$) at 300 hPa during the
719 winters of (a) 1997 and (b) 2002. The crosses denote the centers of action of the
720 AEA pattern.
721 **Figure 10**. Horizontal distribution of 850 hPa wind anomalies (vectors; $m\ s^{-1}$) and
722 divergence (shading; $10^{-5}s^{-1}$) at 700 hPa during the winters of (a) 1997 and (b)
723 2002.
724 **Figure 11**. The spatial distribution of the vertically integrated wet deposition flux
725 anomalies during the winters of (a) 1997 and (b) 2002. (c)-(d), As in (a)-(b), but
726 for the anomalous distribution of aerosol concentrations when the wet deposit is
727 turned off.
728

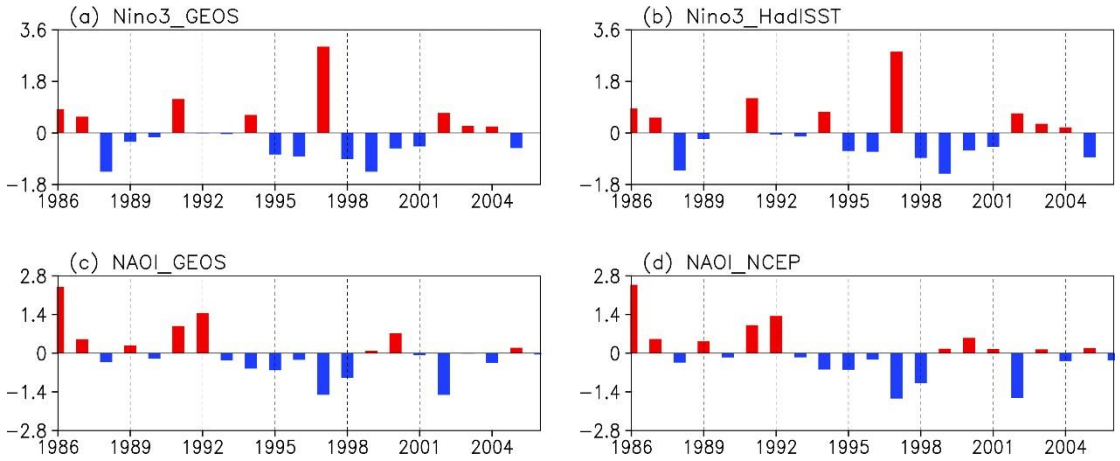

729

730 **Figure 1**. (a) The time series of the Niño3 index based on the GEOS-4 input skin
731 temperature data for 1986-2006 (°C). (b) is similar to (a) but is based on the HadISST.
732 (c) The time series of the NAO index based on the GEOS-4 input sea level pressure. (d)
733 is similar to (c) but is based on the NCEP/NCAR reanalysis.

734

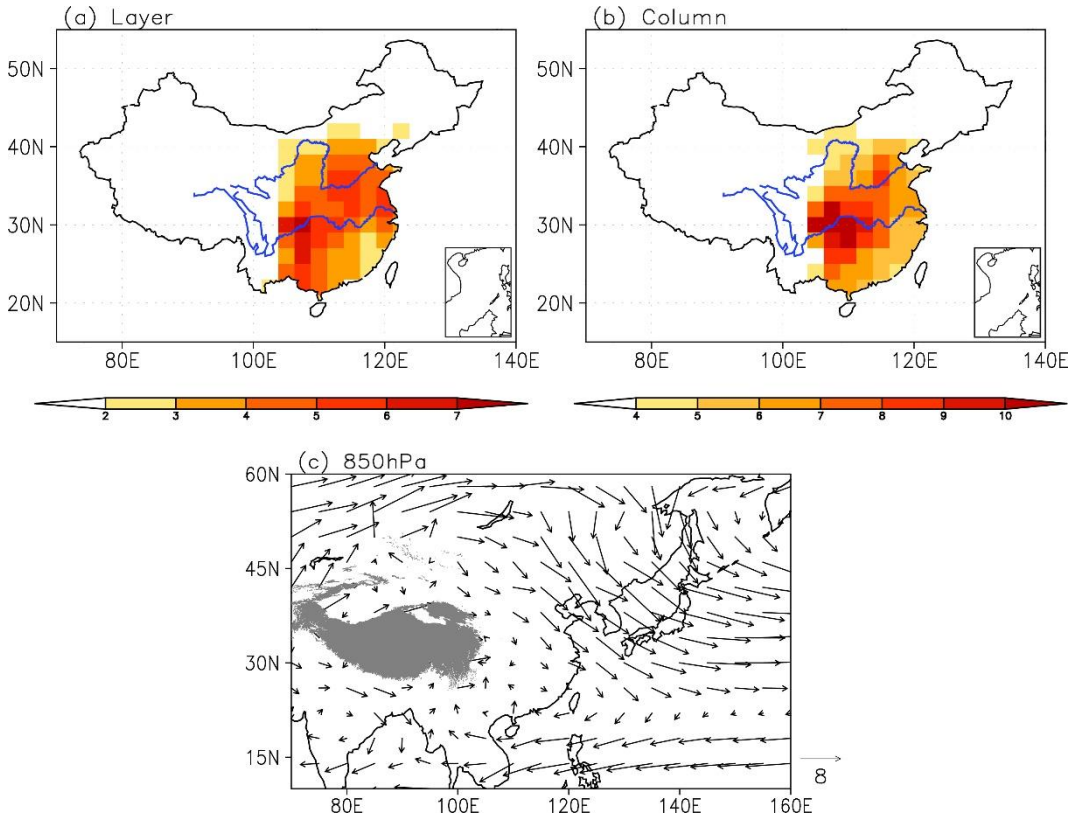

735

736 **Figure 2**. The standard deviation of the simulated (a) surface layer $PM_{2.5}$ concentrations
737 ($\mu g \cdot m^{-3}$) and (b) column burdens of $PM_{2.5}$ ($mg \cdot m^{-2}$) during boreal winter averaged from
738 1986 to 2006. (c) The horizontal distribution of boreal winter climatological mean wind
739 at 850 hPa ($m \cdot s^{-1}$), shaded indicates the Tibetan Plateau.

740

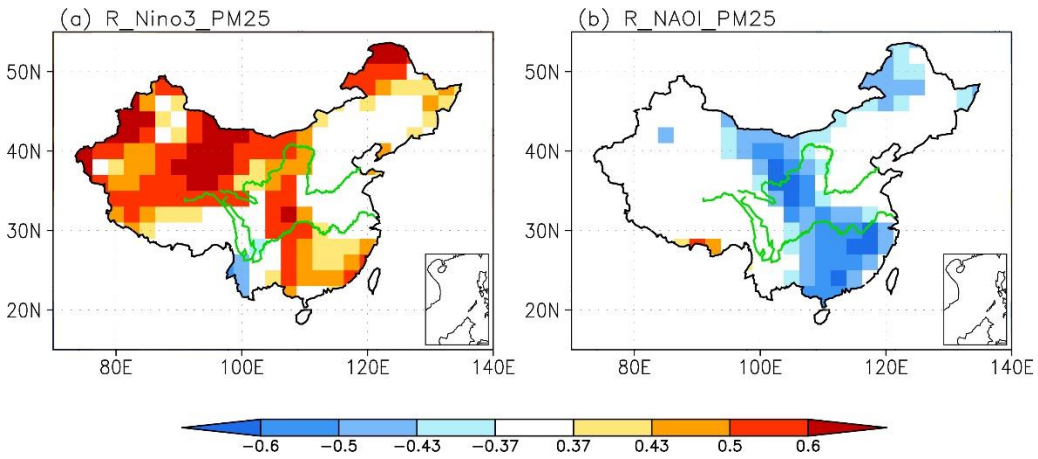

741

742 **Figure 3**. (a) The spatial distribution of the correlation coefficients between surface
743 layer $PM_{2.5}$ concentrations and the Niño3 index. (b) As in (a), but for the correlations
744 with the NAOI. Color shading indicates a significant correlation at the 0.1 level (0.37
745 is the critical value for significance at the 0.1 level).

746

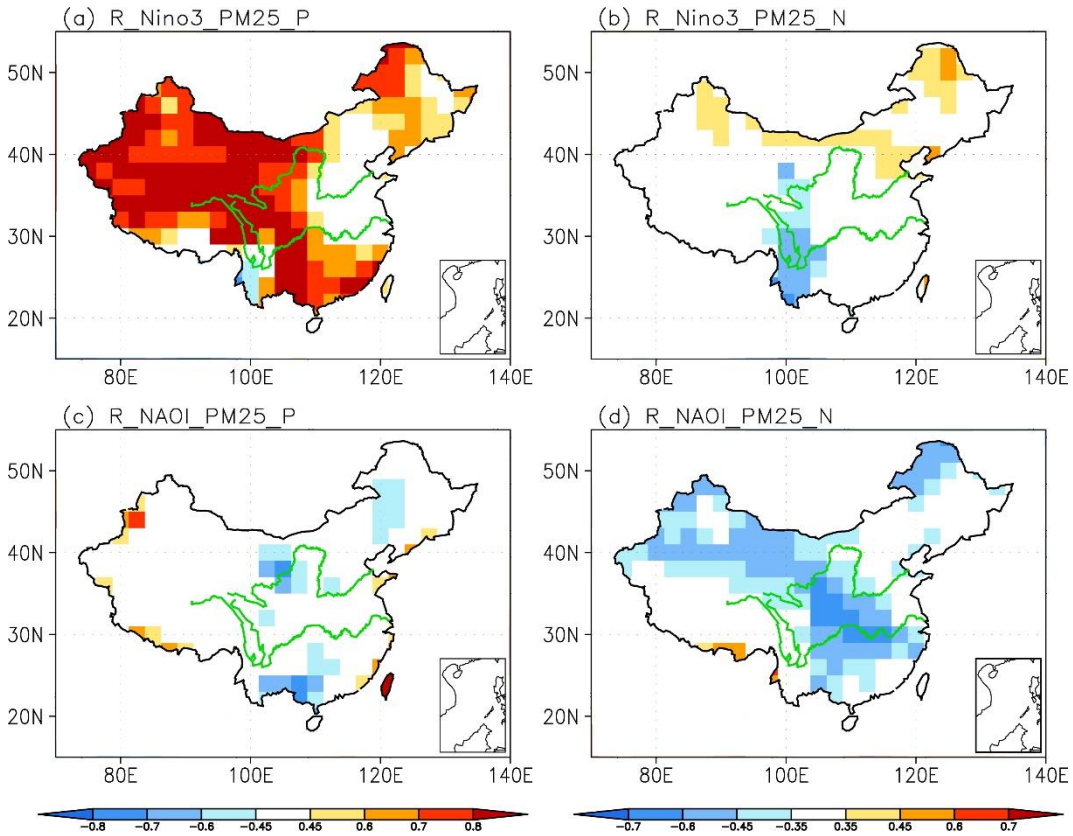

747

748 **Figure 4**. Spatial distribution of the correlation coefficients between (a) positive and (b)
749 negative Niño3 index values and surface-layer $PM_{2.5}$ concentrations. (c)-(d) as in (a)-
750 (b), but for the NAOI. Color shading indicates a significant correlation, (0.35 and 0.45
751 are the critical value for significance at the 0.2 and 0.1 level, respectively).

752

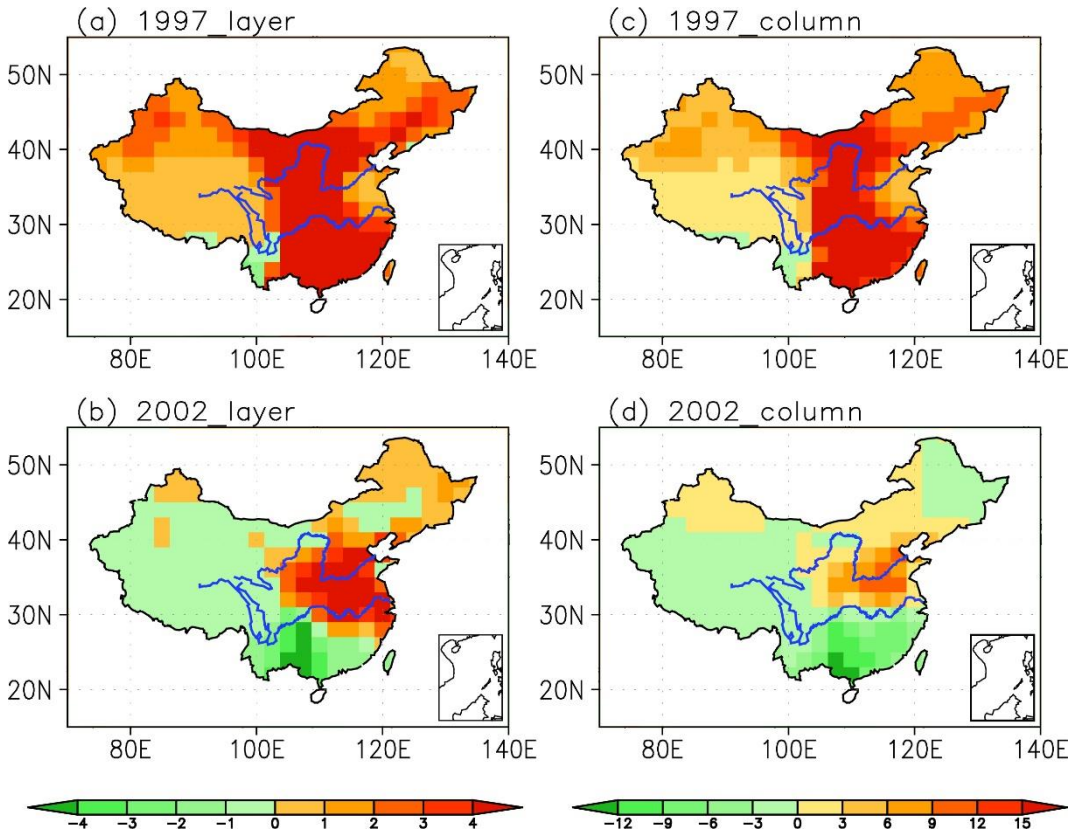

753

754 **Figure 5**. The spatial distribution of the simulated (left panel) anomalous surface layer

755 $PM_{2.5}$ concentrations ($\mu g \cdot m^{-3}$) and (right panel) column burdens of $PM_{2.5}$ ($mg \cdot m^{-2}$)

756 during the boreal winters of 1997 (upper) and 2002 (below).

757

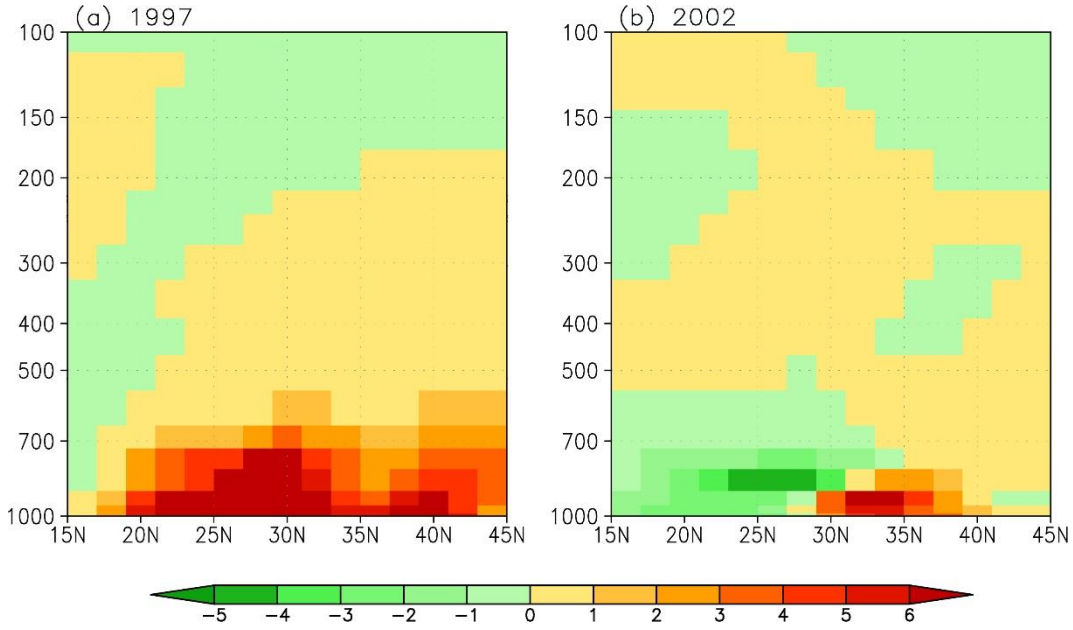

758

759 **Figure 6**. The pressure–latitude distribution of zonally averaged $PM_{2.5}$ anomalies over

760 105°–120°E during the winters of (a)1997 and 2002 ($\mu g \cdot m^{-3}$).

761

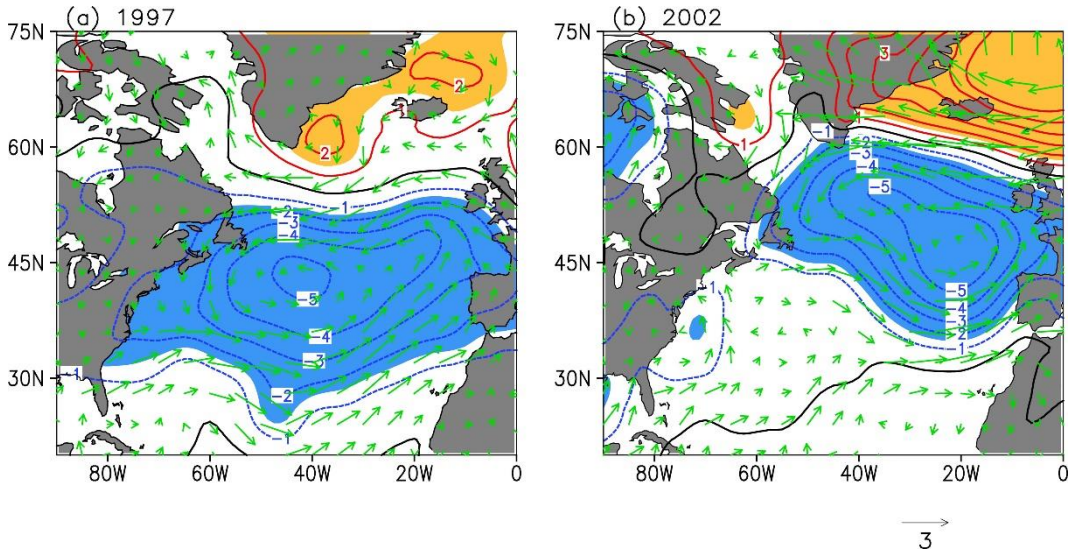

762

763 **Figure 7**. The horizontal distribution of surface wind ($m \cdot s^{-1}$) and surface level pressure

764 (hPa) based on the assimilated meteorological data during the autumns of (a) 1997 and

765 (b) 2002.

766

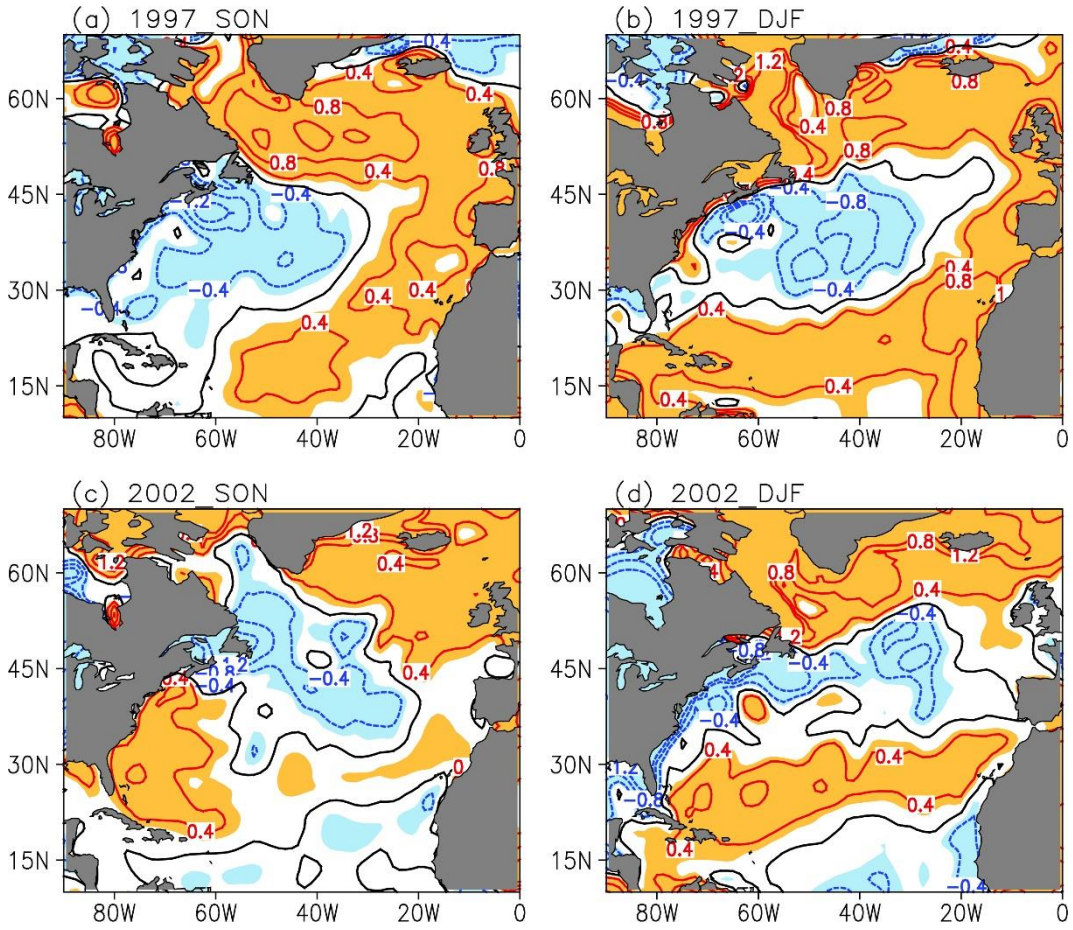

767

768 **Figure 8**. The horizontal distribution of skin temperature anomalies (°C) based on the
769 assimilated meteorological data during the (a) autumn and (b) winter of 1997. (c)-(d)
770 As in (a)-(b), but during 2002.

771

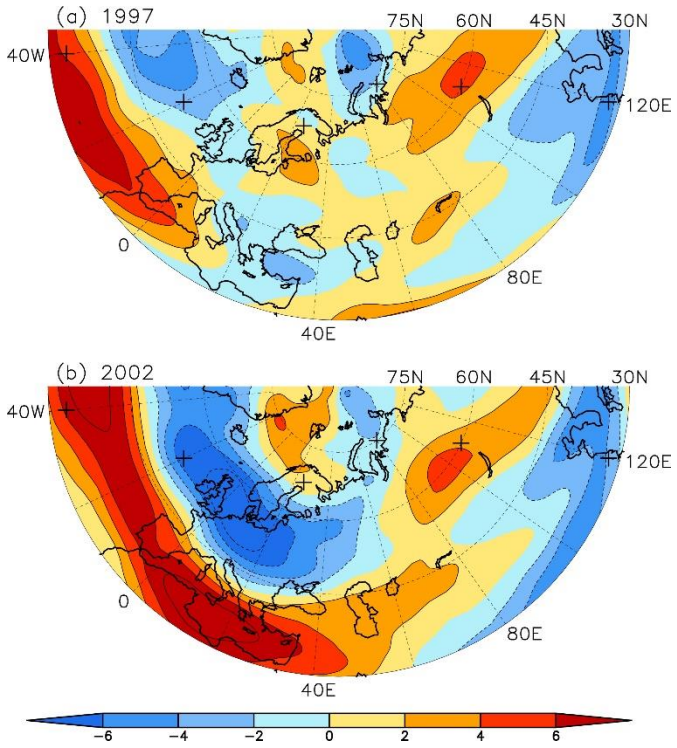

772

773 **Figure 9**. Horizontal distribution of the divergence ($10^{-5}s^{-1}$) at 300 hPa during the
774 winters of (a) 1997 and (b) 2002. The crosses denote the centers of action of the AEA
775 pattern.

776

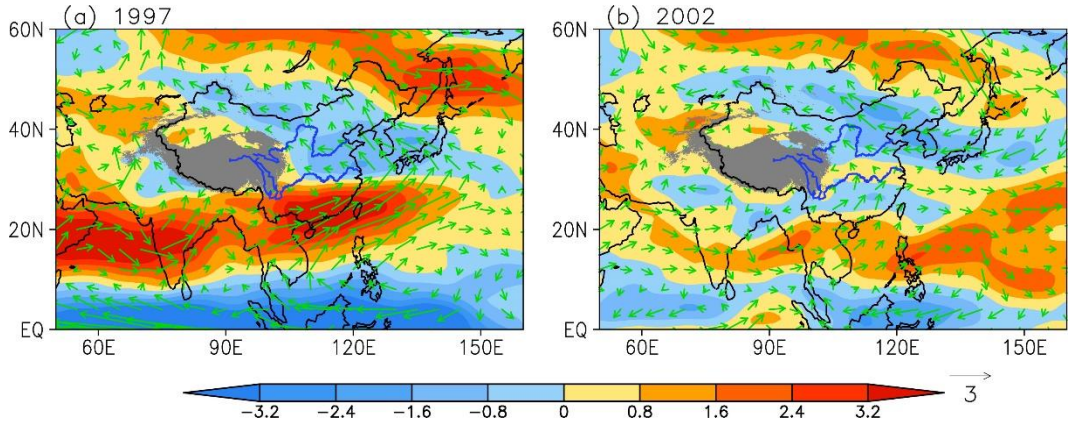

777

778 **Figure 10**. Horizontal distribution of 850 hPa wind anomalies (vectors; m s^{-1}) and

779 divergence (shading; $10^{-5}s^{-1}$) at 700 hPa during the winters of (a) 1997 and (b) 2002.

780

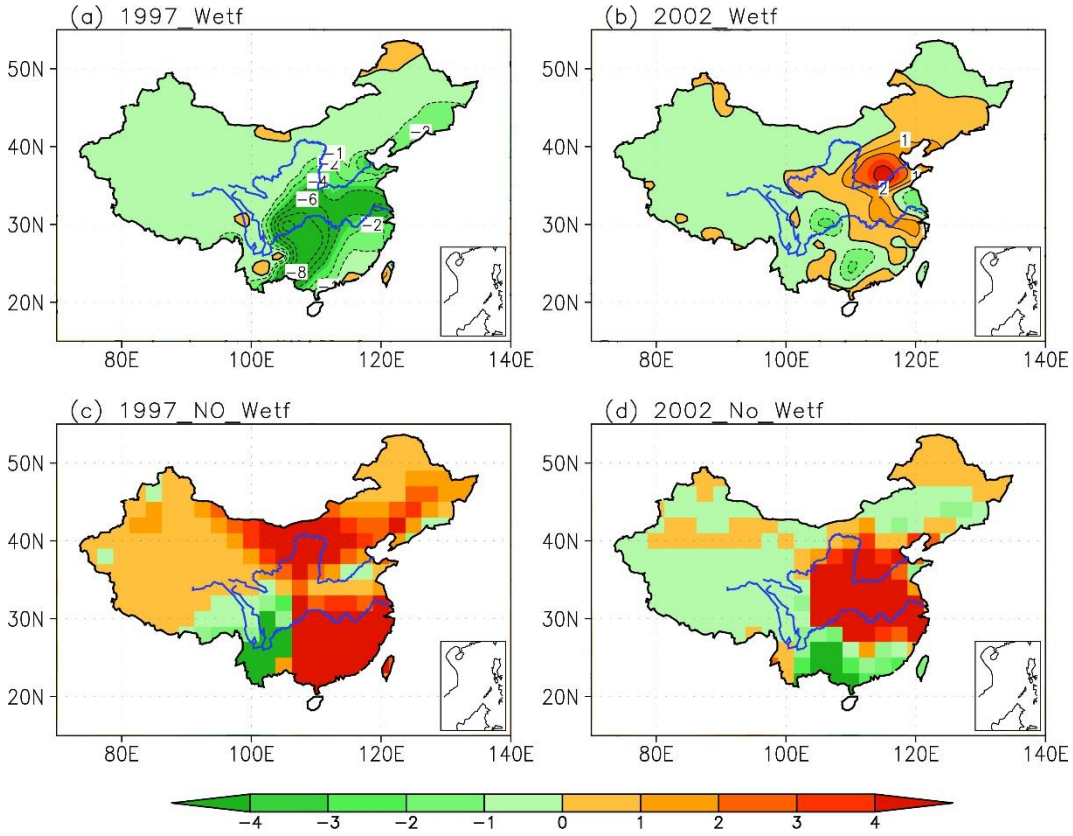

Figure 11. The spatial distribution of the vertically integrated wet deposition flux anomalies during the winters of (a) 1997 and (b) 2002. (c)-(d), As in (a)-(b), but for the anomalous distribution of aerosol concentrations when the wet deposit is turned off.